

## Polarization Switching Dynamics Governed by the Thermodynamic Nucleation Process in Ultrathin Ferroelectric Films

J. Y. Jo,<sup>1</sup> D. J. Kim,<sup>1</sup> Y. S. Kim,<sup>1</sup> S.-B. Choe,<sup>1</sup> T. K. Song,<sup>2</sup> J.-G. Yoon,<sup>3</sup> and T. W. Noh<sup>1,\*</sup>

<sup>1</sup>*FPRD, Department of Physics and Astronomy, Seoul National University, Seoul 151-747, Korea*

<sup>2</sup>*School of Nano Advanced Materials, Changwon National University, Changwon, Gyeongnam 641-773, Korea*

<sup>3</sup>*Department of Physics, University of Suwon, Suwon, Gyeonggi-do 445-743, Korea*

(Received 3 May 2006; published 15 December 2006)

In most ferroelectrics, the domain nucleation barrier ( $U^*$ ) is thermally insurmountable; this is called “Landauer’s paradox.” However, we showed that, in ultrathin films, the large depolarization fields could lower  $U^*$  to a level comparable to thermal energy ( $k_B T$ ), resulting in power-law decay of polarization. We empirically found a universal relation between the power-law decay exponent and  $U^*/k_B T$ . This relation will provide a practical but fundamental limit for capacitor-type ferroelectric devices, analogous to the superparamagnetic limit for magnetic memory devices.

DOI: [10.1103/PhysRevLett.97.247602](https://doi.org/10.1103/PhysRevLett.97.247602)

PACS numbers: 77.22.Ej, 77.80.Dj, 77.80.Fm, 85.50.-n

Recent advances in complex oxide thin film synthesis and in first principles calculations have intensified the basic research on ferroelectricity at nanoscale dimensions [1,2]. Many workers have reported intriguing physical phenomena occurring in ultrathin ferroelectric (FE) films, such as intrinsic size effects [1–3], strain-enhanced FE properties [4], unusual low-dimensional phases [5], and domain patterns [6,7]. On the other hand, the mechanism and domain dynamics of FE switching in ultrathin films have rarely been investigated in spite of their scientific and technological importance [8–10].

Historically, the mechanism of polarization switching dynamics in FEs has been the subject of a great deal of research. It is now believed that polarization switching takes place via the nucleation and growth of new domains [8–10]. However, there still remains an unsolved issue: How do the domains nucleate? In the late 1950s, Landauer emphasized that a thermodynamic nucleation process cannot play a role in FE domain switching [11]. For domain reversal, an energy barrier ( $U^*$ ) for domain nucleation should be thermally overcome, as shown in Fig. 1(a). However, Landauer’s and later estimates showed that  $U^*$  is practically insurmountable by the thermal energy ( $k_B T$ ):  $U^* > 10^8 k_B T$  at an electric field  $E \sim 1$  kV/cm (a typical value of the coercive field for bulk FEs) [11] and  $U^* \sim 10^3 k_B T$  at  $E \sim 100$  kV/cm (a typical value of the coercive field for most FE thin films) [10,12]. This problem has been known as “Landauer’s paradox.” To avoid this paradox, numerous workers have assumed that the nuclei could be formed inhomogeneously due to defects [13], long-range interaction between nuclei [12], and FE-electrode coupling [14]. In this Letter, we will demonstrate that  $U^*$  could be thermally overcome in the ultrathin FE film. The thermodynamic nucleation of reversed domains due to a large depolarization field ( $E_d$ ) could play an important role in the polarization switching process of ultrathin BaTiO<sub>3</sub> films. The thermally activated switching process will be shown to

impose a practical but fundamental limit for capacitor-type FE devices.

Fully strained SrRuO<sub>3</sub>/BaTiO<sub>3</sub>/SrRuO<sub>3</sub> capacitors of high quality were fabricated using pulsed laser deposition [1]. The thickness of BaTiO<sub>3</sub> ( $d_{\text{BTO}}$ ) is between 5.0 and 30 nm. We were able to directly measure polarization-electric field hysteresis loops and polarization decay behaviors even for a 5.0 nm thick BaTiO<sub>3</sub> film [1,15,16]. As shown in Fig. 2(a), these SrRuO<sub>3</sub>/BaTiO<sub>3</sub>/SrRuO<sub>3</sub> capacitors with a  $10 \times 10 \mu\text{m}^2$  area displayed an intriguing time-dependent polarization decay behavior, which was measured using electric write or read pulses separated by a given decay time ( $t$ ) [9,15], as schematically displayed in the inset in Fig. 2(b). Figure 2(a) shows that the polarization decay follows a power-law behavior at room temperature [15]: namely,  $\Delta P(t) \sim t^{-n}$ . As the film becomes thinner, the value of  $n$  increases substantially. In particular, for the 5.0 nm thick capacitor,  $\Delta P$  decays below 1% of its initial value within  $10^{-3}$  s. This rapid polarization decay must be caused by domain backswitching upon removal of  $E$  and is the subject of the discussions that follow.

With uniform polarization in the capacitor geometry, the discontinuity of polarization at the FE-electrode interfaces

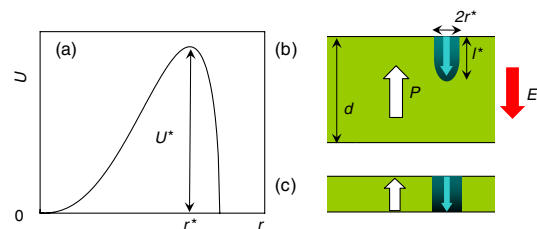


FIG. 1 (color online). (a) A schematic diagram of electrostatic energy ( $U$ ) for the nucleus formation as a function of the nuclear radius ( $r$ ). Schematic diagrams of (b) the half-prolate spheroidal nucleus formation and (c) the cylindrical nucleus formation, with reversed polarization.

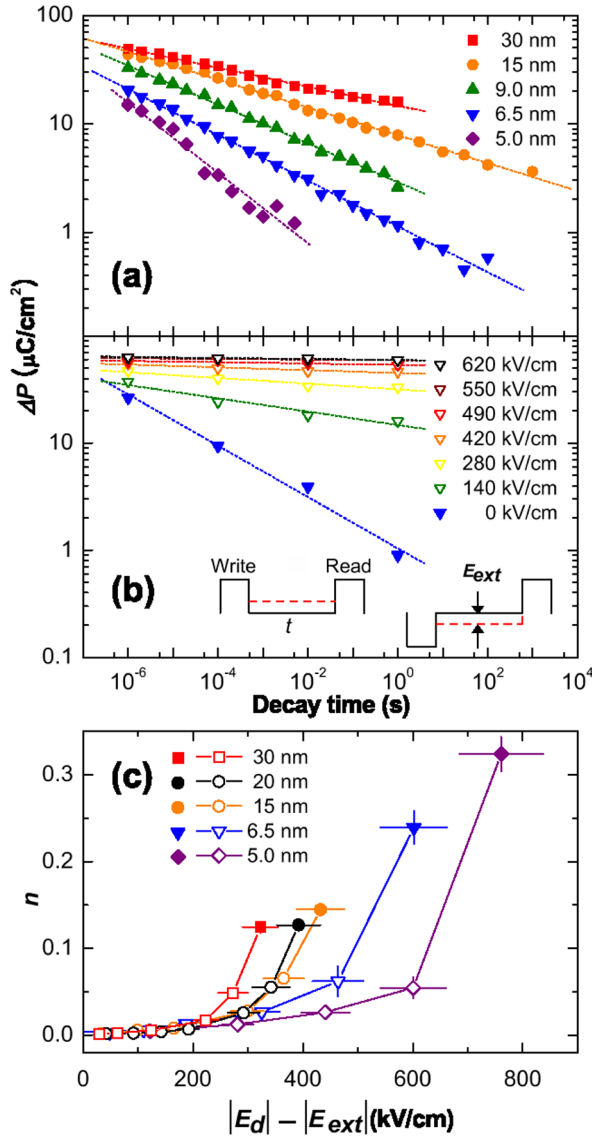


FIG. 2 (color online). (a) Time-dependent net polarization changes  $\Delta P(t)$  without any external field ( $E_{\text{ext}}$ ). (b)  $\Delta P(t)$  of the 6.5 nm thick BaTiO<sub>3</sub> capacitor under numerous values of  $E_{\text{ext}}$ . The left- and right-hand diagrams of the inset show electric pulse trains used to measure nonswitching and switching polarizations, respectively.  $\Delta P(t)$  corresponds to the difference between these polarizations. (c) The relation between  $n$  and  $(|E_d| - |E_{\text{ext}}|)$ . The open and solid symbols correspond to the data with and without  $E_{\text{ext}}$ , respectively.

induces polarization bound charges. The free carriers inside the electrodes compensate these bound charges. However, the finite value of the Thomas-Fermi screening length for the free carriers makes the compensation incomplete, resulting in  $E_d$  inside the FE layer [17]. It should be noted that the generation of  $E_d$  is inevitable, which will limit the performance of most FE capacitor-type devices.

To investigate effects of  $E_d$  on the polarization decay, we measured the  $t$  dependence of  $\Delta P$  with an external static field ( $E_{\text{ext}}$ ), applied in the opposite direction to that of  $E_d$ , displayed schematically by the dashed red lines in the inset

in Fig. 2(b) [15]. Since  $E_{\text{ext}}$  will partially cancel out  $E_d$ , it will slow down the polarization decay and consequently reduce the values of  $n$ . As shown in Fig. 2(b),  $n$  decreases significantly with an increase of  $E_{\text{ext}}$  and should finally become zero when  $E_{\text{ext}}$  becomes nearly the same as  $E_d$ . This  $E_{\text{ext}}$  value at  $n \sim 0$  provides an experimental value for lower limit of  $E_d$  [15]. For the 6.5 nm thick BaTiO<sub>3</sub> film,  $E_d$  can be as large as 600 kV/cm.

Figure 2(c) shows the dependence of  $n$  on  $(|E_d| - |E_{\text{ext}}|)$ , for the BaTiO<sub>3</sub> capacitors. The abscissa values of the solid symbols, which were measured with  $E_{\text{ext}} = 0$ , correspond to the experimentally estimated  $E_d$  values. They clearly show that  $E_d$  becomes larger as  $d_{\text{BTO}}$  becomes smaller. As the  $(|E_d| - |E_{\text{ext}}|)$  increases, the value of  $n$  increases for all samples. However, we could not find any simple universal relation between  $n$  and  $(|E_d| - |E_{\text{ext}}|)$  with this plot.

Note that a decrease of  $\Delta P$  means an increase in the volume of FE domains with a reversed polarization. It is generally believed that the growth of the opposite domains occurs in three processes, namely, (a) formation of nuclei with opposite polarization, (b) their forward growth, and (c) sidewise growth (called domain wall motion). For epitaxial FE films thicker than 100 nm, domain wall motion has been reported to be very important [10]. However, for ultrathin FE films, domain wall motion becomes extremely slow: For example, the speed of the domain wall motion was estimated to be about 1 nm/s for a 29 nm thick Pb(Zr, Ti)O<sub>3</sub> film under  $E \sim 1000$  kV/cm [8]. In addition, the forward growth of the nuclei is known to occur very quickly (i.e., a speed of 1000 m/s) [9], so the very slow domain wall motion could not play a major role in the polarization decay behavior observed in Fig. 2(a). Therefore, we propose that, in the ultrathin FE films, the rapid polarization decay should be governed by nucleation of domains.

Figures 1(b) and 1(c) schematically display formation of nuclei with half-prolate spheroidal and cylindrical shapes, respectively, under  $E$ . Here  $d$  is the FE film thickness, and  $r^*$  and  $l^*$  represent the critical radius and length of the half-prolate spheroidal nucleus, respectively. Kay and Dunn calculated the electrostatic energy ( $U$ ) for such nuclei formation and showed that  $U^*$  is proportional to  $\sigma_w^3/E^{5/2}$  for the half-prolate spheroidal nucleus and  $\sigma_w^2/E$  for the cylindrical nucleus, where  $\sigma_w$  is the domain wall energy [18]. When  $l^* < d$ , the half-prolate spheroidal nuclei are likely to be formed. Using electrostatic calculation [18], the crossover from the half-prolate spheroidal to cylindrical shapes will occur at  $d \sim 15$  nm [19]. The experimental  $E_d$  values of our BaTiO<sub>3</sub> films are between 300 and 800 kV/cm [15]. With these  $E_d$  values, the  $U^*/k_B T$  values are estimated to be between 4 and 20 at room temperatures, which are easily accessible by thermal energy, allowing thermally activated domain nucleation.

To investigate how the thermally activated nucleation process can cause the observed power-law decay behavior,

we used numerical simulations adopting the Monte Carlo algorithm [20]. We approximated the film to be composed of  $128 \times 128$  single domain cells lying on the  $ab$  plane, whose size corresponding to critical nuclei is 2.0 nm and height is the same as the film thickness, with a periodic boundary condition. Each cell has a uniform polarization ( $P$ ), pointing either up or down along the  $c$  axis. The dimensionless parameter  $x$  ( $\equiv P/P_s$ ) was set to be either +1 or -1 to describe the bistable nucleus states, where  $P_s$  is spontaneous polarization. During the switching process, the Hamiltonian ( $H^i$ ) per volume ( $V^i$ ) of the  $i$ th cell can be expressed as a function of the  $i$ th value of  $x^i$ :

$$H^i = -K_2(x^i)^2 - \frac{\sigma_w d_{\text{BTO}}}{2V^i} x^i \sum_{\text{nn}} r_{\text{nn}}^i x_{\text{nn}}^i - E_d^i \cdot P_s x^i - E_{\text{ext}} \cdot P_s x^i. \quad (1)$$

The first self-energy term is quite similar to the leading  $P^2$  term in the Landau-Devonshire equation [21]. The second term describes the short-range wall interaction between the nearest neighboring domains, where  $r_{\text{nn}}$  and  $x_{\text{nn}}$  are the adjacent circumference and unit vector of nearest neighbor domain cells, respectively. The third term originates from the long-range dipolar interaction between cells. The dipolar field ( $E_d^i$ ) is the sum of the dipolar electric field caused by all of the other cells. The last term describes the work done by an external source.

When two electrodes sandwich a FE film, the electrode screens the value of  $E_d^i$  produced by  $P_s$ . The screening can occur not only in the perpendicular direction but also in the lateral direction. A numerical estimate reveals that the lateral screening length should be of the order of  $d$ . For an ultrathin FE film, only the dipolar interaction between the nearest neighbor domains across domain boundaries could be important, so  $E_d^i$  can be approximated to  $\hat{e}_d \sum_{\text{nn}} r_{\text{nn}}^i x_{\text{nn}}^i$ , where  $\hat{e}_d$  is the line density of the dipolar field across the cell boundary. Then Eq. (1) can be rewritten as

$$H^i = -K_2(x^i)^2 - \frac{\sigma_w^{(\text{eff})} d_{\text{BTO}}}{2V^i} x^i \sum_{\text{nn}} r_{\text{nn}}^i x_{\text{nn}}^i - E_{\text{ext}} \cdot P_s x^i, \quad (2)$$

where an effective wall energy density  $\sigma_w^{(\text{eff})}$  can be defined as  $\sigma_w^{(\text{eff})} = \sigma_w + \hat{e}_d P_s 2V^i / d_{\text{BTO}}$ . The analytic form of the screened dipolar interaction energy term is identical with that of the domain wall energy. The simulations were performed at room temperature with  $K_2 = 3 \times 10^6$  J/m<sup>3</sup> [21] and an attempt frequency of  $10^9$  Hz. The  $\sigma_w$  value in the literatures is varied between 3 and 17 mJ/m<sup>2</sup> [22–24]. Using  $\sigma_w = 10$  mJ/m<sup>2</sup> [24], we estimated  $\sigma_w^{(\text{eff})} = -1$  mJ/m<sup>2</sup>. The cell size agrees with the domain nuclei size calculated on the basis of electrostatic nucleation model [11] and is comparable to that of the first principles theory [7]. The experimentally obtained value from Ref. [15] was used for  $P_s$ .

The Monte Carlo simulations with dipolar interaction between domains showed a power-law behavior of polarization decay. Without changing any other parameter val-

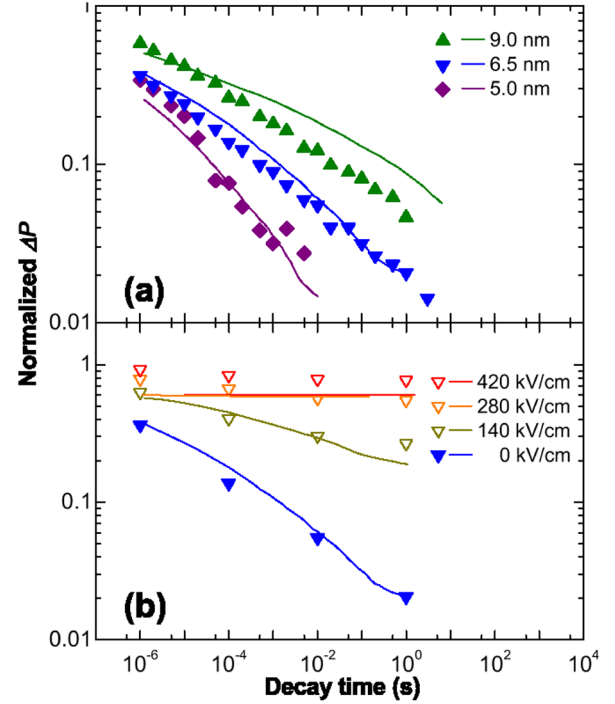


FIG. 3 (color online). (a) Normalized  $\Delta P(t)$  without any  $E_{\text{ext}}$ . (b) Normalized  $\Delta P$  of the 6.5 nm thick BaTiO<sub>3</sub> capacitor under numerous values of  $E_{\text{ext}}$ . The symbols and lines correspond to the experimental data and the Monte Carlo simulation results, respectively.

ues, we performed the same simulations for other thicknesses of BaTiO<sub>3</sub> capacitors and found reasonably good agreement, as shown in Fig. 3(a). We also performed similar simulations for the cases with nonzero values of  $E_{\text{ext}}$  and obtained good agreement with experimental data, as shown in Fig. 3(b) [19].

Our results show that, in our BaTiO<sub>3</sub> ultrathin films, homogeneous nucleation could occur by thermal activation without invoking the defect-mediated inhomogeneous nucleation mechanism. The Landauer's paradox may be no longer an important issue in ultrathin films. In our simulation, the inclusion of small amount of defects only caused the overall shift of decay time, but the power-law behavior in polarization decay remained intact.

If the thermodynamic domain nucleation is the governing process for polarization decay,  $U^*/k_B T$  should be the most important physical term which determines the decay exponent ( $n$ ). According to Kay and Dunn [18],  $U^* \sim \sigma_w^3 / (|E_d| - |E_{\text{ext}}|)^{5/2}$  for half-prolate spheroidal nucleation and  $U^* \sim \sigma_w^2 / (|E_d| - |E_{\text{ext}}|)$  for cylindrical nucleation, by substituting  $(|E_d| - |E_{\text{ext}}|)$  instead of  $E$ . As shown in the inset in Fig. 4,  $U^*/k_B T$  decreases with the increase of  $(|E_d| - |E_{\text{ext}}|)$ .

We found empirically a universal relation between  $n$  and  $U^*/k_B T$ . As shown in Fig. 4, all values of  $n$  fall onto a single scaling curve, regardless of  $d_{\text{BTO}}$  and  $(|E_d| - |E_{\text{ext}}|)$ . Comparison with Fig. 2(c) indicates that  $U^*/k_B T$  could be an important physical parameter which describes the ob-

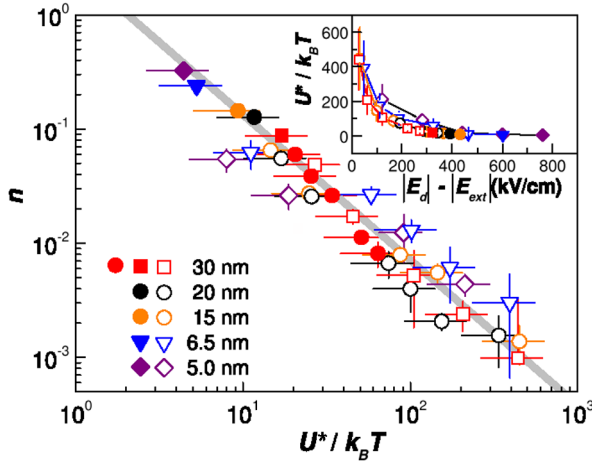


FIG. 4 (color online). A scaling relation between  $n$  and  $U^*/k_B T$ . The open and solid symbols come from the experimental  $\Delta P(t)$  data with and without  $E_{\text{ext}}$ , respectively. The inset shows the relation between  $U^*/k_B T$  and  $(|E_d| - |E_{\text{ext}}|)$ .

served polarization decay process. To further confirm the importance of  $U^*/k_B T$ , we independently performed polarization decay measurements for the 30 nm thick BaTiO<sub>3</sub> capacitor at various temperatures. The solid red circles in Fig. 4 correspond to the experimental data for temperature-dependent polarization decay, which fall onto the seemingly universal line between  $n$  and  $U^*/k_B T$ . This universal scaling with  $U^*/k_B T$  points out that the polarization switching process should be governed by thermodynamic nucleation process. Further experimental and theoretical investigations on polarization decay are desirable for ultrathin FE films of other material systems than BaTiO<sub>3</sub>.

The empirical relation between  $n$  and  $U^*/k_B T$  has some important implications for the design of nanoscale FE devices. Namely, the polarization decay due to  $E_d$  could impose a new fundamental thickness limit on such FE devices. For example, FE random access memories require the retention of a certain value of  $\Delta P$  for 10 years [9]. For our BaTiO<sub>3</sub> capacitors,  $U^*$  should be higher than  $40k_B T$  to retain  $\Delta P$  at more than 50% of the initial value ( $n < 0.02$ ). This value of  $U^*$  corresponds to a thickness of about 40 nm for our fully strained BaTiO<sub>3</sub> films, which is much thicker than the critical thickness (2.4 nm) for the ferroelectricity of BaTiO<sub>3</sub> [2]. For ultrathin film capacitors, a condition of  $U^* \geq A \cdot k_B T$ , where  $A$  is a constant of the order of 10, has to be satisfied in order to have a stable retention property. As the  $E_d$  value increases (decrease in  $U^*$ ) with the reduction of  $d_{\text{BTO}}$ , retention loss due to the thermodynamic nucleation of reversed domains becomes much more severe. Note that this situation is analogous to that of the superparamagnetic limit for magnetic memory devices: A long-range ferromagnetic order vanishes when anisotropy energy becomes comparable to thermal fluctuation energy [25].

In conclusion, we have addressed three important issues related to polarization switching in FE ultrathin films.

(i) We showed that the domain dynamics in ultrathin BaTiO<sub>3</sub> films should be governed by the thermally activated nucleation process with Landauer's paradox being no longer an important issue in this regime. (ii) We found empirically a universal relation between the polarization decay exponent and the domain nucleation energy barrier, regardless of film thickness, applied electric field, and temperature. (iii) The simple universal relation can provide a guide for device design. There can be a practical but fundamental thickness limit for capacitor-type devices, whose effect is analogous to the superparamagnetic limit in magnetic systems.

We thank M.W. Kim for discussion. This work was financially supported by Creative Research Initiatives of MOST/KOSEF.

\*Electronic address: twnoh@snu.ac.kr

- [1] Y. S. Kim *et al.*, Appl. Phys. Lett. **86**, 102907 (2005).
- [2] J. Junquera and P. Ghosez, Nature (London) **422**, 506 (2003).
- [3] D. D. Fong *et al.*, Science **304**, 1650 (2004).
- [4] K. J. Choi *et al.*, Science **306**, 1005 (2004).
- [5] H. N. Lee *et al.*, Nature (London) **433**, 395 (2005).
- [6] I. Kornev *et al.*, Phys. Rev. Lett. **93**, 196104 (2004).
- [7] Bo-Kuai Lai *et al.*, Phys. Rev. Lett. **96**, 137602 (2006).
- [8] T. Tybell *et al.*, Phys. Rev. Lett. **89**, 097601 (2002).
- [9] J. F. Scott, *Ferroelectric Memories* (Springer-Verlag, New York, 2000).
- [10] Y. W. So *et al.*, Appl. Phys. Lett. **86**, 092905 (2005).
- [11] R. Landauer, J. Appl. Phys. **28**, 227 (1957).
- [12] A. M. Bratkovsky and A. P. Levanyuk, Phys. Rev. Lett. **85**, 4614 (2000).
- [13] A. Aharoni, *Introduction to the Theory of Ferromagnetism* (Clarendon, Oxford, 1996).
- [14] G. Gerra *et al.*, Phys. Rev. Lett. **94**, 107602 (2005).
- [15] D. J. Kim *et al.*, Phys. Rev. Lett. **95**, 237602 (2005).
- [16] Y. S. Kim *et al.*, Appl. Phys. Lett. **88**, 072909 (2006).
- [17] R. R. Mehta *et al.*, J. Appl. Phys. **44**, 3379 (1973).
- [18] H. F. Kay and J. W. Dunn, Philos. Mag. **7**, 2027 (1962).
- [19] Our coercive field data agree quite well with the electrostatic calculation based on nucleation models in Ref. [11]. (The calculation was done using experimental values except for one free parameter  $\sigma_w$ .) In our BaTiO<sub>3</sub> ultrathin films, coercive field data indicated the crossover of nuclei shape from the half-prolate spheroid to cylinder at  $d_{\text{BTO}} \sim 15$  nm. This result also supports the picture of polarization switching dynamics governed by thermodynamic nucleation process in ultrathin films. This result can be found at J. Y. Jo *et al.*, Appl. Phys. Lett. **89**, 232909 (2006).
- [20] S.-B. Choe and S.-C. Shin, IEEE Trans. Magn. **36**, 3167 (2000).
- [21] N. A. Pertsev *et al.*, Phys. Rev. Lett. **80**, 1988 (1998).
- [22] J. Fousek and M. Šafránková, Jpn. J. Appl. Phys. **4**, 403 (1965).
- [23] B. Meyer and D. Vanderbilt, Phys. Rev. B **65**, 104111 (2002).
- [24] W. J. Merz, Phys. Rev. **95**, 690 (1954).
- [25] S. Chikazumi, *Physics of Ferromagnetism* (Oxford University Press, New York, 1997).